Assessing Seal Capacity of Exploited Oil and Gas Reservoirs, Aquifers and Coal Beds for Potential Use in CO_2 Sequestration

Final GCEP Report

Funding Period January 1, 2003 Through August 31st, 2006

Submitted October 31, 2006

Principal Investigator Mark D. Zoback, Professor of Geophysics, Stanford University

Graduate Research Assistants Amie Lucier, Laura Chiaramonte, Hannah Ross, Lourdes Colmenares

Post-doctoral Research Associate Paul Hagin

Assessing Seal Capacity of Depleted Oil and Gas Reservoirs, Aquifers and Coal Beds for Potential Use in CO_2 Sequestration

Investigators

Mark D. Zoback, Professor of Geophysics, Paul Hagin, Research Associate and Hannah Ross and Laura Chiaramonte, Graduate Research Assistants

1.1 Introduction

In this section we review activities carried out during the period of no-cost extension of the 2006 GCEP award. We include the activities and results in the three areas previously reported (GCEP Annual Report, 2006): modeling CO_2 sequestration in coal, evaluation of the feasibility of CO_2 sequestration in a depleted oil field and laboratory measurements on coal shrinkage and swelling.

1.2 Results

1.2.1 CO_2 Sequestration in unmineable coalbeds of the Powder River Basin, Wyoming

We have continued our examination of the feasibility of sequestering CO_2 in unmineable coalbeds by conducting a reservoir characterization study and fluid flow simulations on coalbeds in the Powder River Basin (PRB), Wyoming. In particular, we were interested in the ECBM potential of CO_2 sequestration and modeling the effects of horizontal hydraulic fractures on CO_2 injectivity. Our study focused on the sub-bituminous Big George coal, part of the Wyodak-Anderson coal zone of the Tertiary Fort Union Formation. The main results from this study have been presented in previous GCEP reports. In this section we will describe results from a sensitivity study carried out on the parameters used in the fluid flow simulations. Table 1.1 lists the parameter values for the base case simulation.

Sensitivity Analysis

At present we have carried out a sensitivity study on a number of the model and simulation input parameters, including cleat permeability and porosity, the BHP injector constraint, cleat spacing, cleat compressibility, reservoir pressure, coal thickness, gas diffusion time, and the Palmer and Mansoori (1996; 1998; GEM 2005) parameters. Figure 1.1 shows the results of this sensitivity analysis. We are currently investigating the effect of well spacing, using a horizontal injection well and injecting flue gases on the CO_2 sequestration and ECBM potential of the Big George coal.

Cleat Permeability

Doubling the cleat permeability increased CH_4 production and CO_2 injectivity (Figure 1.1). However, CO_2 breakthrough occurred earlier than in the base case and a larger volume of CO_2 was produced. By increasing the permeability we increased the total gas flow through the cleats. In contrast, halving the permeability reduced CH_4 production and the CO_2 injection rate, but meant that CO_2 breakthrough was negligible (Figure 1.1).

We also looked at the effect of using a homogeneous cleat permeability field compared to a heterogeneous field on total gas volumes injected and produced. Almost all other ECBM simulation studies use a constant cleat permeability, which does not capture the heterogeneous nature of cleat permeabilities in the field. Our simulations show that if we used a homogenous cleat permeability field we would over predict the amount of CO_2 that can be injected and CH_4 that can be produced (Figure 1.1). This suggests that it is better to try and capture the heterogeneity of the coal cleat permeability in the reservoir model or you will over predict the coal's CO_2 sequestration potential.

Cleat Porosity

Halving the cleat porosity increased CH_4 production and CO_2 injectivity, whereas doubling the porosity decreased both CH_4 production and total CO_2 injected (Figure 1.1). By doubling the cleat porosity we introduced more water into the cleats (since we specify that the cleats are water saturated), making it harder for the gas to flow through the cleats and requiring additional water to be produced.

Cleat Spacing

Decreasing the cleat spacing increased both the total CO_2 injected and CH_4 produced (Figure 1.1). Increasing the number of cleats in the model meant that the injection rate could increase because there are more high permeability areas in which the CO_2 can be injected. The higher number of cleats also decreased the diffusion time, which is why a lot more CH_4 could be produced. The faster the diffusion, the faster methane can desorb and flow to the production wells.

It is interesting to note that decreasing the number of cleats in the horizontal direction did not have much of an effect on CO_2 injection volumes or CH_4 production volumes. It seems that the most important pathways to the producer are the vertical cleats.

Maximum Bottom Hole Pressure Injector Constraint

The BHP constraint for the injector had a significant effect on the total volume of CO_2 injected and total CH_4 produced. Increasing the constraint meant that more CO_2 was injected, causing more CH_4 to be desorbed from the matrix in exchange for CO_2 (Figure 1.1).

Gas Diffusion Coefficient

Increasing the gas diffusion coefficient increased both the total volume of CO_2 injected and the total volume of CH_4 produced (Figure 1.1). Increasing the diffusion coefficient meant that adsorption and desorption were faster. More CH_4 was produced because a lot more was able to desorb and flow to the wells within the simulation run time.

Coal Thickness

Halving the coal thickness had the effect of decreasing the total volume of CO_2 injected and CH_4 produced because of the lower initial CH_4 in place and lower coal volume for CO_2 storage (Figure 1.1).

Reservoir Pressure

Increasing the reservoir pressure also decreased the total CO_2 injected, whereas the total CH_4 produced increased (Figure 1.1). The decrease in CO_2 injectivity is because the pore pressure in the reservoir is higher than in the base case, so less gas can be injected. And the increase in CH_4 production is because there is more initial CH_4 adsorbed.

Palmer and Mansoori Paramters

Cleat compressibility and strain at infinite pressure are included in the Palmer and Mansoori equation (Palmer and Mansoori, 1996; 1998; GEM 2005) that calculates cleat permeability changes due to desorption and adsorption of gases in the coal matrix and changes in effective pressure. We found that by decreasing the cleat compressibility we decreased both the total volume of CO_2 injected and the total volume of CH_4 produced because it became harder to open the cleats (they became stiffer) and therefore increase permeability (Figure 1.1).

The Palmer Mansoori parameter "volumetric strain at infinite pressure" is a measure of the volume change in the coal matrix due to the adsorption and desorption of gases, and can be fit by a Langmuir curve (Harpalani, 2005). A higher strain means that there is a greater change in matrix volume, and if that change is an increase in volume, then the permeability reduction will be large, reducing injectivity and production. This is what we observe when we increase the volumetric strain for CO_2 (Figure 1.1). However, when we increase the volumetric strain for CH_4 we see an increase in both CO_2 injection and CH_4 production, which means that there has been a large, negative change in the matrix volume because of desorbing CH_4 (decrease in volume), so matrix shrinkage dominates in this case and cleat permeability increases (Figure 1.1).

Young's modulus, Poisson's ratio and the exponent used to relate cleat porosity and permeability are also included in the Palmer and Mansoori equation, but from Figure 1.1 we can see that CO_2 injection and CH_4 production are not very sensitive to these parameters.

Table 1.1: Input parameters for the fluid flow base case simulation.

Input Parameters	Values	References
Initial temperature, °C	22	Tang et al. (2005)
Reservoir pressure gradient, kPa/m	7.12	Advanced Resources International, Inc. (2002)
Coal gas composition	90% CH_4, 0% CO_2, 10% N_2	
Water saturation	99% in cleats, 0% in matrix	Advanced Resources International, Inc. (2002)
Injector BHP constraint, kPa	4000	
Producer BHP constraint, kPa	1000	History-matching
Cleat spacing, cm	10	Flores (2004), Ayers (2002)
Matrix permeability, mD	0.04-0.7	Flores (2004)
Matrix porosity	0.011-0.1	Advanced Resources International, Inc. (2002)
Cleat permeability, mD	Horizontal face cleat direction, 7-152, horizontal butt cleat direction, 1-48 and vertical direction, 1-48	Literature (Flores et al., 2004; Twombly, et al., 2004; Mavor et al., 2003; Ayers, 2002; Laubrach et al., 1998; USGS, 1995), and history-matching
Cleat porosity	0.023-0.208	Literature (Twombly, et al., 2004; Mavor et al., 2003; Advanced Resources International, Inc., 2002; USGS, 1995) and history-matching
Adsorption/desorption parameters for PRB coal samples (dry coal desorption for CH_4 and N_2 and moist coal adsorption for CO_2)	Langmuir volume: 0.577 gmol/kg for CH_4, 1.67 gmole/kg for CO_2	Tang et al. (2005)
	Inverse Langmuir pressure, 1.7E-3/kPa for CH_4, 8.5E-4/kPa for CO_2	
Diffusion coefficient, cm^2/s	0.000001 (100 days) for CH_4 and CO_2	GCEP Technical Report (2004)
Rock compressibility	Rock compressibility, 1.45E-7/kPa for matrix and 2.9E-5/kPa for cleats	Law et al. (2003) for matrix and USGS (1995) for cleats
	Reference pressure, 2246 kPa for matrix and cleats	
Shrinkage/swelling (Palmer and Mansoori, 1996; 1998) for modified Palmer and Mansoori equation in GEM 2005	Strain Langmuir pressure for CH_4, 2069 kPa and CO_2, 345 kPa	Harpalani (2005)
	Young's modulus, 0.413E7 kPa	Jones et al. (1998)
	Poisson's ratio, 0.39	Jones et al. (1988)
	Strain at infinite pressure for CH_4, 0.007 and CO_2, 0.013	Harpalani (2005)
	Exponent, 3	Palmer and Mansoori (1996; 1998)
S_3, kPa	6200	Colmenares and Zoback (in press)

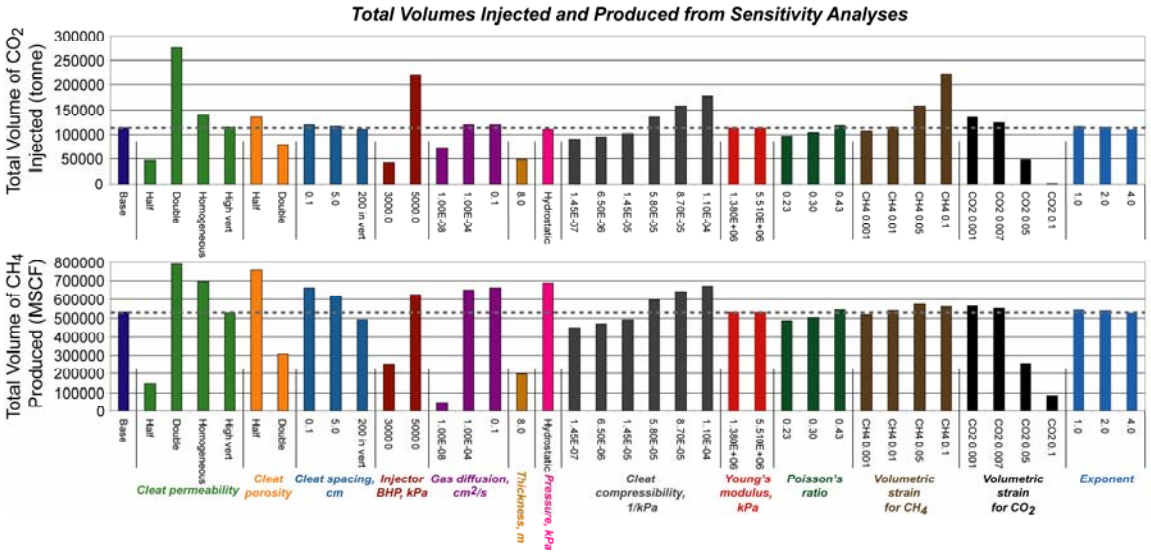

Figure 1.1: Total volumes of CO_2 injected and CH_4 produced due to changes in the model and input parameters for the fluid flow simulations. Cleat compressibility, Young's modulus, Poisson's ratio, matrix volumetric strain and the exponent used to relate cleat porosity and permeability are all included in the Palmer and Mansoori (1996; 1998; GEM 2005) equation. The dark blue boxes correspond to the base case, and the values used for the parameters in the base case are listed in Table 1.1. All of these simulations incorporate matrix shrinkage and swelling, but no hydraulic fracture.

1.2.2 The Stability of Sealing Faults in the Teapot Dome field

A comprehensive geomechanical model for the Tensleep Fm. was generated in the context of providing the technical foundation required for the Rocky Mountain Oilfield Testing Center (RMOTC) and its partners to consider and design a CO_2 injection project at Teapot Dome. This model allows the project team to quantitatively estimate the pore pressure at which the S1 fault would slip, and therefore supports predictions about the risk of leakage in the target storage unit.

As reported previously, we found that at the depth of the Tensleep Fm. (red line in Fig. 1.3) approximately 17 MPa of excess pressure would be required to cause the fault to slip. This pressure corresponds to a CO_2 column height of approximately 2500 m (at a density = 700 kg/m^3). As the structural closure of the Tensleep Fm. in this area is no more than 100 m, we established that the S1 fault is not at risk of reactivation and becoming a possible leakage pathway for CO_2 migration.

During the no-cost extension of this project, we used Quantitative Risk Assesment to formally evaluate how uncertainties in the horizontal principal stress (S_{hmin} and S_{Hmax}) magnitudes, as well as uncertainties of the strike and dip of the fault (due to limits on seismic resolution and time-depth conversion) affect the slip potential of the S1 fault.

Random distributions of S_1, S_2, and S_3 were generated based on the mean, minimum and maximum stress values estimated in each well. For simplicity, Normal Fault ($S_1=S_v$, $S_2=S_{Hmax}$ and $S_3=S_{hmin}$) and Strike-Slip ($S_1=S_{Hmax,}$ $S_2=S_v$ and $S_3=S_{hmin}$) cases were analyzed separately using over 3000 Monte Carlo Simulations. Figure 1.2 (for normal faulting) and Figure 1.3 (for strike-slip faulting) show the fault slip probability as a function of reservoir pressure for variations of the indicated component of the stress tensor (the others remaining fixed). From this analysis it was established that in 99.9% of the cases the pressure at which slip on the S1 fault would be induced is above 14 MPa.

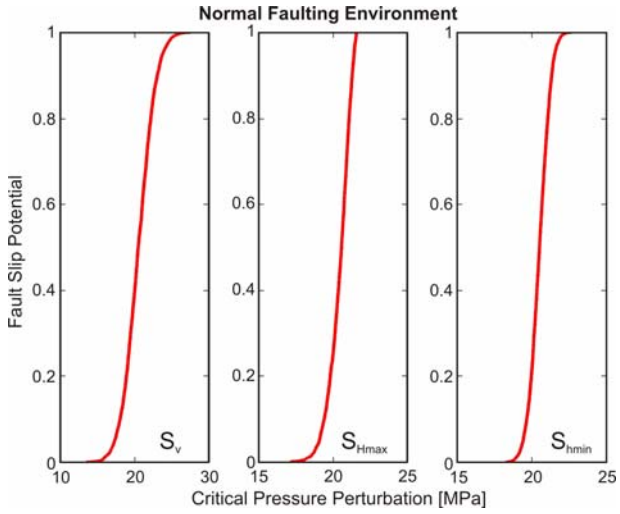

Figure 1.2: Fault slip potential probability for Normal Fault environment, as function of each of the components of the stress tensor, varying S1 (maintaining S2 and S3 fixed) (left); varying S2 (maintaining S1 and S3 fixed) (center) and varying S3 (maintaining S1 and S2 fixed) (right).

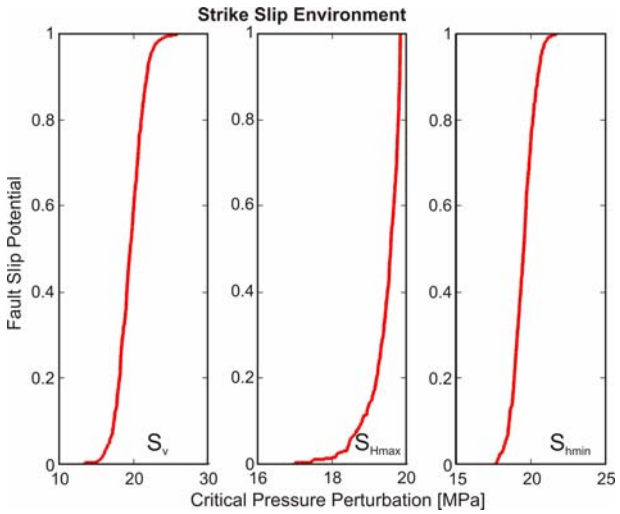

Figure 1.3: Fault slip potential probability for Strike-Slip environment, as function of each of the components of the stress tensor, varying S1 (maintaining S2 and S3 fixed) (left); varying S2 (maintaining S1 and S3 fixed) (center) and varying S3 (maintaining S1 and S2 fixed) (right).

To account for the uncertainties in the geometry of the fault, Figure 1.4 illustrates the fault slip potential probability as a function of variations in the azimuth (Fig. 1.4, left) and dip of the fault (Fig. 1.4, right). These cases where evaluated with the mean values of the stress tensor. Even though the biggest impact in the fault slip potential is function of the uncertainty in the dip, for 99.9% of the cases considered, the pressure perturbation values are above 10 MPa.

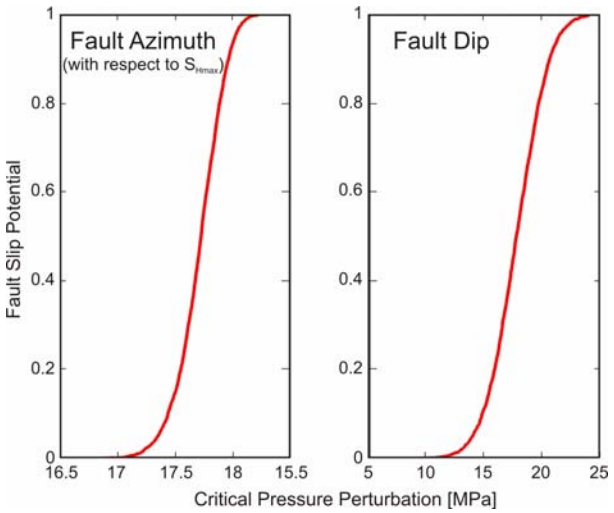

Figure 1.4 Fault slip potential probability as function of variation in the fault azimuth (left) and in the fault dip angle (right). The mean value of the stress tensor was used to analyze these scenarios.

Conclusions

A comprehensive Quantitative Risk Assesment for the Tensleep Fm. was performed in the context of providing the technical foundation required for the RMOTC and its partners to consider and design a CO_2 injection project at Teapot Dome. The components of the stress tensor as well as the geometry of the fault were subjected to a sensitivity analysis, from what it was established that in the more pessimistic scenario (lower values of fault dip) 99.9% of the cases, at the depth of the target horizon, it would require approximately 10 MPa of excess pressure to cause the S1 fault to reactivate. This value could be achieved by a CO_2 column height of approximately 1500 m. As the average closure of the Tensleep Fm. structure in this area does not exceed 100 m, the S1 fault does not appear to be at risk of reactivation and therefore providing a leakage pathway for CO_2 under the present stress field.

Planned refinements to this analysis are direct measurements of S_{hmin} to be taken in the Tensleep Fm. as well as in the caprock; these will provide more reliable estimates of maximum sustainable pressures before hydrofracturing the caprock, and the maximum CO_2 column height that this structure could support. The sensitivity analysis highlighted the influence of the fault dip angle in the P_{cp} estimation, therefore refining the time-depth conversion model to accurately estimate the dip of the fault is also essential. Accounting

for other faults, under the seismic resolution, will have to be determined, either from FMI interpretation and well correlation, or from surface reservoir analogs.

1.2.3 Laboratory Studies of Coal Shrinkage and Swelling

To date, efforts in the laboratory have been focused on modifying and adding equipment to optimize the apparatus for measuring the physical and chemical properties of coal. Specifically, flow controllers, new pore fluid lines, and a gas analyzer were added to the apparatus, so that gas permeability could be measured during coal shrinkage and swelling experiments. The existing fluid permeability setup remains fully functional, and both the gas and fluid pore lines can be used simultaneously, so it will be possible to study fluid substitution effects or two-phase flow. The temperature control setup was modified to improve its accuracy and provide greater stability over long periods of time. As described below, this was necessary because each experiment is expected to run for several weeks. Modifications and the necessary system calibrations were completed in October 2006, and experiments are currently underway. The new laboratory system can be seen in schematic form in Figure 1.5. A detailed view of the new permeability system and sample coreholders is provided in Figure 1.6.

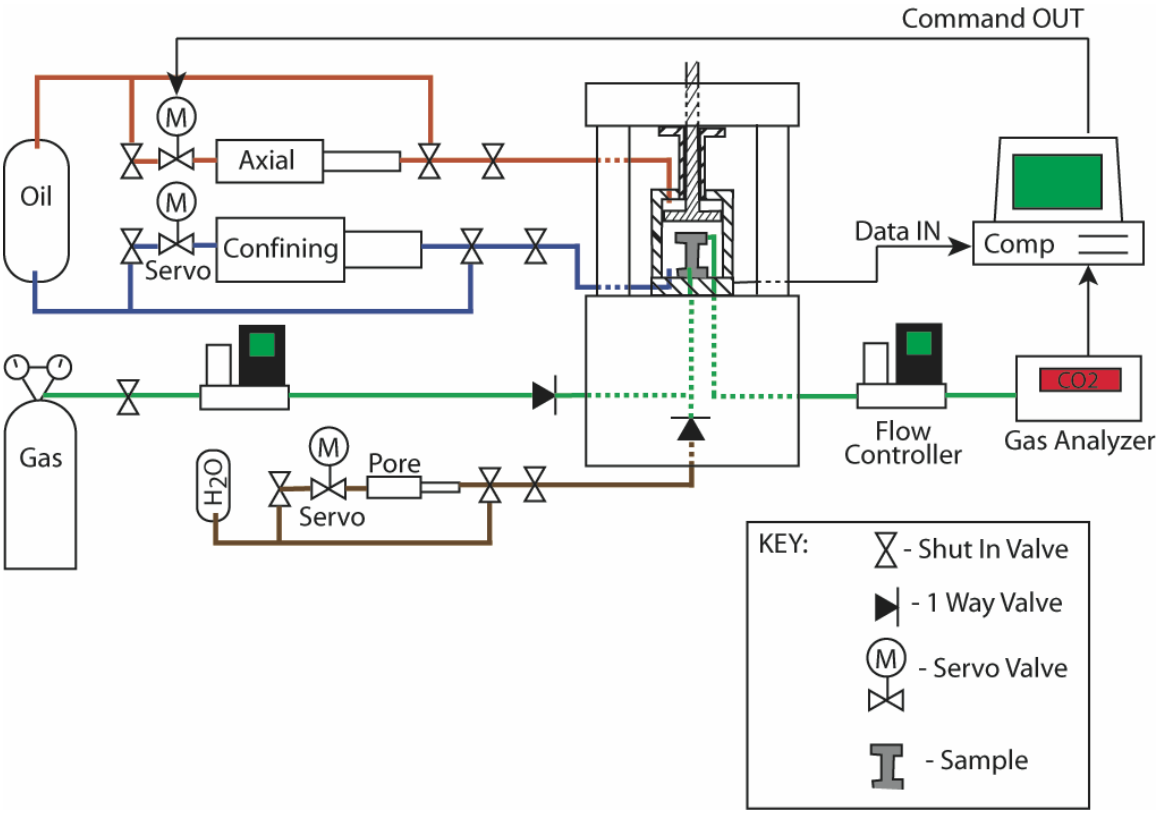

Figure 1.5: Schematic view of the completed laboratory apparatus. Items connected by the green hydraulic lines (Gas canister, flow controllers, analyzer) represent the new equipment added to the system.

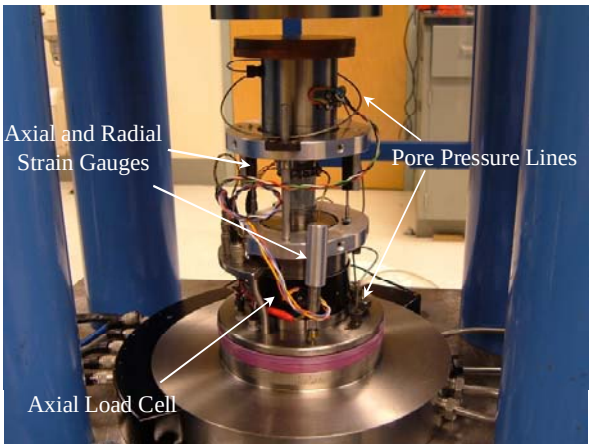

Figure 1.6: Photograph showing modified coreholder assembly, including new pore pressure lines for gas permeability measurements. A coal sample core can be seen in the center of the coreholder assembly, jacketed in Teflon heatshrink tubing.

The experimental plan was changed from the original plan proposed last year, in order to better integrate with the laboratory studies being performed by other groups (Anthony Kovscek and Jerry Harris), and to provide better constraints on the input parameters going into the numerical modeling studies of enhanced coal bed methane and CO_2 sequestration in coal beds. The current experimental plan is shown in Figure 1.7, and consists of the following three phases: 1) baseline measurements of physical properties (static, dynamic, and permeability) in the presence of an inert gas (Helium), 2) measurements of shrinkage/swelling and the associated effect on permeability in the presence of methane or carbon dioxide, and 3) measurements of coal plasticity as a function of temperature. Because it has been difficult to obtain intact core samples from the Powder River Basin coal, the experimental plan has been designed to derive as much information as possible from each sample. Each of these phases is described in more detail below.

1) Numerical results from the Powder River Basin (PRB) case study suggest that both methane production and CO_2 injectivity are sensitive to the elastic properties of the coal. The first phase of our experimental plan has been designed to measure the elastic properties of coal. Bulk modulus, Young's modulus, and Poisson's ratio will be measured both statically (2 axial LVDTs and 1 radial chain gauge), and dynamically (ultrasonic P and S waves at 1 MHz) as a function of effective stress. Helium permeability will be measured simultaneously with deformation, at a constant pore pressure of 300 psi. As shown in Figure 1.7, effective stress on the samples will be increased at a constant rate, although several holds are planned during loading, to ensure that time-dependent plastic deformation is not occurring.

2) Coal beds are unique among gas reservoirs, because the physical properties of coal change as a function of the gasses adsorbed to the coal matrix. We are

interested in knowing how the physical properties of coal change during desorption of CH_4 and adsorption of CO_2. During Phase 2 of the experimental plan, we will measure the shrinkage and swelling of the coal matrix in response to adsorbing CH_4 or CO_2, and then repeat the loading history of Phase 1, to study the effect of adsorbed gas on the elastic properties of the coal. While numerical results from the PRB case study suggest that matrix swelling due to CO_2 adsorption has a minor effect on cleat permeability, the results assumed that the Palmer-Mansoori equation is valid. We plan to test this assumption in the laboratory, and modify the equation if necessary to refine the numerical results.

3) Finally, during Phase 3 of the experiment, we plan to increase the temperature of the pressure vessel using an insulated heating coil, and repeat the loading history from Phase 1, to investigate the potential effects of plasticity on gas permeability and velocity. Temperatures will range from 50 to 100 C, to simulate *in situ* conditions. If plasticity is observed, static plastic moduli will be measured, and a full elastic-plastic failure envelope will be constructed for the coal. Plasticity can have a potentially large impact, particularly if CO_2 decreases the plastic transition temperature. It is anticipated that plasticity would increase the compressibility of the cleats, thereby decreasing the cleat permeability.

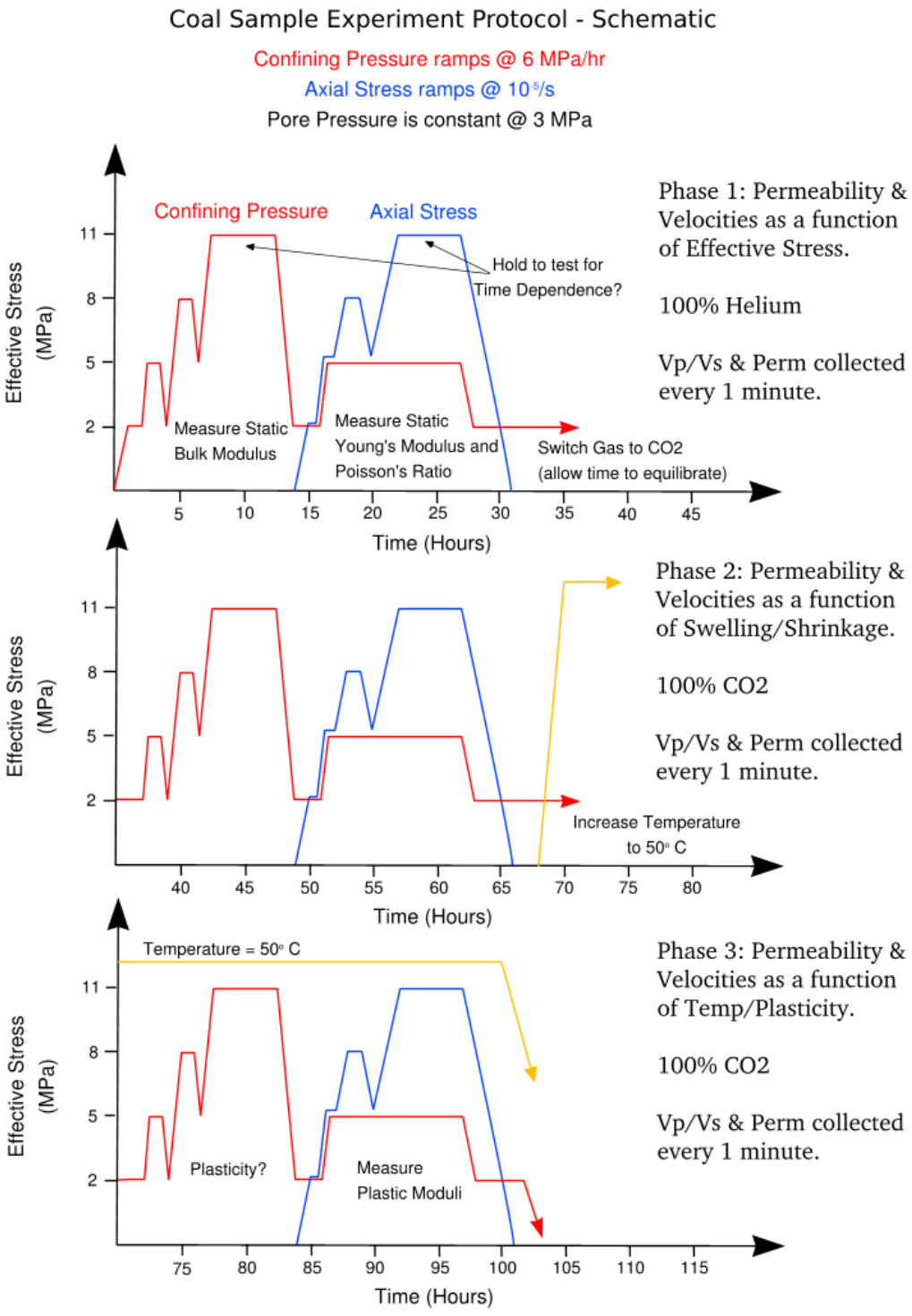

Figure 1.7: Schematic diagram describing the experimental plan for the Powder River Basin coal samples. Both powdered and intact coal samples will be tested following this general procedure. See the text for details.

1.3 Publications and Conferences

1. Chiaramonte, L., Zoback, M., Friedmann, J. and Stamp, V. Seal Integrity and Feasibility of CO2 Sequestration in the Teapot Dome EOR Pilot: Geomechanical Site Characterization. Journal of Environmental Geology (accepted for publication after minor revisions, 2006).

2. Chiaramonte, L., Zoback, M., Friedmann, J. and Stamp, V., The potential for fault reactivation associated with CO2 sequestration in the Teapot Dome Field, Wyoming. Stanford Rock Physics and Borehole Geophysics Annual Meeting, Stanford, CA, June 26-28.

3. Chiaramonte, L., Zoback, M., Friedmann, J. and Stamp, V., CO2 Sequestration, Fault Stability and Seal Integrity at Teapot Dome, Wyoming. GCEP Symposium, September 18 – 20, 2006, Stanford University, CA

4. Lucier, A., Zoback, M., Gupta, N. and Ramakrishnan, T. S.. Geomechanical aspects of CO2 sequestration in a deep saline reservoir in the Ohio River valley region. Environmental Geosciences, volume 13, number 2, pages 85-103, June 2006.

5. Lucier, A., Zoback, M, Gupta N. and Ramakrishnan, T.S. Geomechanical aspects of CO2 sequestration near coal burning power plants in the Midwestern United States. Greenhouse Gas Control Technologies Conference 8, Trondheim, Norway, June 19-22.

6. Lucier, A., Zoback, M. Geomechanical aspects of CO2 sequestration in a deep saline reservoir in the Ohio River valley region. Stanford Rock Physics and Borehole Geophysics Annual Meeting, Stanford, CA, June 26-28

7. Ross, H. E. and Zoback, M. D., 2006, CO2 sequestration and ECBM in coalbeds of the Powder River Basin, Wyoming: Reservoir simulation and sensitivity analyses: presented at the Stanford Rock Physics and Borehole Geophysics Annual Meeting, Stanford, CA, June 26-28.

1.4 References

1. Advanced Resources International, Inc., 2002, Powder River Basin coalbed methane development and produced water management: DOE/NETL-2003/1184.
2. Ayers, W., 2002, Coalbed gas systems, resources, and production and a review of contrasting cases from the San Juan and Powder River basins: AAPG Bulletin, 86, 1853-1890.
3. Colmenares, L. B. and Zoback M. D., in press, Hydraulic fracturing and wellbore completion of coalbed methane (CBM) wells in the Powder River Basin, Wyoming: Implications for water and gas production: AAPG Bulletin.
4. Flores, R. M., 2004, Coalbed methane in the Powder River Basin, Wyoming and Montana: An assessment of the Tertiary-Upper Cretaceous coalbed methane total petroleum system: U.S. Geological Survey Digital Data Series, DDS-69-C, chapter 2.
5. Harpalani, S., 2005, Gas flow characterization of Illinois coal: Final technical report, ICCI project number 03-1/7.1B-2.
6. Harpalani, S. and Chen, G., 1997, Influence of gas production induced volumetric strain on permeability of coal: Geotechnical and Geological Engineering, 15, 303-325.
7. Jones, A. H., Bell, G. J. and Schraufngel, R. A., 1988, A review of the physical and mechanical properties of coal with implications for coalbed methane well completion and production: Coal-bed Methane, San Juan Basin, Rocky Mountain Association of Geologists, 169-181.
8. Laubrach, S. E., Marrett, R. A., Olson, J. E. and Scott, A. R., 1998, Characteristics and origins of coal cleat: A Review: International Journal of Coal Geology, 35, 175-207.
9. Law, D. H. –S., van der Meer, L. G. H. and Gunter, W. D., 2003, Comparison simulators for greenhouse gas sequestration in coalbeds, part III: More complex problems: 2nd Annual Conference on Carbon Sequestration, May 5-8.

10. Mavor, M. J., Russell, B. and Pratt T. J., 2003, Powder River Basin Ft. Union coal reservoir properties and production decline analysis: SPE 84427.
11. Palmer, I. and Mansoori, J., 1996, How Permeability Depends on Stress and Pore Pressure in coalbeds: A New Model: SPE 36737, Proceedings of the 71st Annual Technical Conference, Denver, CO.
12. Palmer, I., and Mansoori, J., 1998, How Permeability Depends on Stress and Pore Pressure in Coalbeds: A New Model: SPE 52607, SPEREE, 539-544.
13. Stanford University Global Climate and Energy Project (GCEP), 2004, Technical Report 2003-2004: <http://gcep.stanford.edu/pdfs/technical_report_2004.pdf>.
14. Tang, G.-Q., Jessen, K. and Kovscek, A.R., 2005, Laboratory and simulation investigation of enhanced coalbed methane recovery by gas injection: SPE 95947.
15. Twombly, G., Stepanek, S. H. and Moore, T. A., 2004, Coalbed methane potential in the Waikato Coalfield of New Zealand: A comparison with developed basins in the United States: 2004 New Zealand Petroleum Conference Proceedings.
16. U. S. Geological Survey National Oil and Gas Resource Assessment Team, 1995, 1995 National assessment of United States oil and gas resources: U. S. Geological Survey Circular 1118.

1.5 Contacts

Laura Chiaramonte: chiarlau@pangea.stanford.edu
Paul Hagin: hagin@pangea.stanford.edu
Amie Lucier luciera@pangea.stanford.edu
Hannah Ross: hemiller@pangea.stanford.edu
Mark Zoback: zoback@pangea.stanford.edu